HTTPS://DOI.ORG/10.48047/AFJBS.6.SI4.2024.4958-4971

African Journal of Biological Sciences

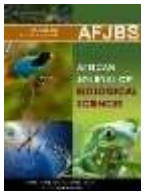

Green Synthesis Of Fe@Carbon Dot Nanocomposites Using Euphorbia Heterophylla: Exploring Sustainable Synthesis, Characterization And Biological Activities.

K Siva Lova Krishna[1&2], Dasari Kalyani[2*], B Nageshwari[1*]

[1]Department of Biotechnology, Government College (Autonomous), Rajamahendravaram, India
[2]School of Life and Health Sciences, Adikavi Nannaya University, Rajahmundry, India

***Corresponding Authors:** Dr. B. Nageshwari, Prof. D. Kalyani
*Emails: b.nageshwari@gcrjy.ac.in, dk.zoo@aknu.edu.in.

Article History
Volume 6, Issue 4s, August 2024
Received: 5 Aug 2024
Accepted: 10 Aug 2024
Published: 20 Aug 2024
doi:10.48047/AFJBS.6.Si4.2024.4958-4971

Abstract:
Nanoparticles, particularly carbon dots (CDs), have gained prominence in biological research due to their distinctive properties. CDs, a novel class of nanomaterials with metal-free fluorescent attributes, are especially noteworthy. Biomass-derived CDs exhibit low toxicity, biocompatibility, and eliminate the need for additional doping or surface modifications. In this study, CDs were synthesized from Euphorbia heterophylla using a sand bath-assisted method, demonstrating their unique capabilities as reducing agents for the synthesis of Fe@EHCDs nanocomposites. The optical and fluorescence properties of CDs confirmed the successful formation of Fe@EHCDs nanocomposites. Fourier-transform infrared (FTIR) analysis elucidated the functional groups present in CDs and Fe@EHCDs nanocomposites. The size distribution of Fe@EHCDs nanocomposites ranged between 2-8 nm. Notably, among the tested pathogens, only Candida albicans exhibited susceptibility to Fe/EHCDs nanocomposites, with a minimum inhibitory concentration (MIC) of 250 µg mL^{-1} and a zone of inhibition of 18 mm at 2000 µg mL^{-1}. Furthermore, the study explored the *in vitro* antioxidant and anti-inflammatory properties of the synthesized nanocomposites. Among the three assessed biological activities, the *in vitro* antioxidant activity displayed particularly promising results.

Keywords: Carbon dots, Green synthesis, Biomass, FeNP's, *Euphorbia heterophylla*, Biological properties.

INTRODUCTION:

The pressing global issues related to energy, the environment and health have spurred the development of innovative materials and methodologies aimed at conserving energy, fostering a sustainable ecosystem, and enhancing human wellbeing[1].

Carbon dots (CD's) (or) Carbon quantum dot's [CQD's] are novel class of quasi spherical, tunable carbon nanoparticles with size <10nm and contains conjugated sp^2 carbon core, oxygen [In the form

multiple oxygen containing functional groups e.g. hydroxyl, carboxyl, epoxy, ether and aldehydes] and other heteroatoms as dopants [2]. Due to their photostability, strong and tunable fluorescence, quantum yield, hydrophilic nature, biocompatibility, low cost, eco-friendliness, and low toxicity, their applications enables a broad range of scientific fields such as bioimaging, optoelectronics, biosensing, photocatalysis, drug delivery and biolabeling etc.[3-5].Recently, many of the studies has been carried out to understand potential applications of CD's, and synthesis methods require expensive and non- renewable carbon source, toxic solvents, high reaction time and temperature etc.[6].

Green chemistry approaches for the synthesis of CD's using natural sources such as biomass and biowastes have attracted researchers due to economical, facile and sustainable routes[7].Utilizing biomass as a carbon source for synthesis of CD's proves advantageous given its eco-friendly nature compared to conventional carbon sources[8].Biomass offers cost-effectiveness, ease of accessibility, environmental friendliness and highly abundant making it a preferred choice for CD's synthesis. Moreover, the process transforms low value biomass waste into valuable and useful materials[9].

Plants are one of the important renewable biomass sources and globally available precursor material for the synthesis of CD's. The inherent presence of biomolecules and phytochemicals in plants eliminates the necessity for doping agents, surface modification, and post-modification of CDs[10]. Plant derived CDs exhibit distinctive properties, serving as adept electron donors and acceptors, and additionally, they function as effective reducing agents than corresponding plant extracts for the synthesis of metal/metal oxide nanoparticles. However the luminescence properties of CDs are depend upon the pH, temperature and excitation wavelength[11]. Among all other metallic nanoparticles, Metallic iron and Iron oxide nanoparticles are of great interest because of their less toxicity towards life and environment. Synthesis of iron nanomaterials using green approach represents a significant stride in the advancement of nanomaterials [12].

Euphorbia heterophylla (Linn.) belongs to the Euphorbiaceae family and used in the treatment of various human ailments which is endemic to subtropical and tropical regions of United States and introduced to tropical Africa and Asian countries[13]. Recent studies has been carried out for the synthesis of Ag/TiO2 [14], Ag/HZSM-5 nanocomposites [15], ZnO [16], rGO [13], Co3O4 [17], MnO_2[18], and NiO [19] nanoparticles using *Euphorbia heterophylla* extract as reducing, capping and stabilizing agent.

However, CD's are effective in reducing metal/metal oxide nanoparticles, the present study aims to use the CD's derived from *Euphorbia heterophylla* for reduction of FeNP's. The Antimicrobial, *Invitro* antioxidant and *invitro* anti-inflammatory properties of Fe@EHCD'S are carried out.

2. Materials and Methods:

2.1. Collection of Plant Material: The whole *Euphorbia heterophylla* (EH) plant was collected from Adikavi Nannaya University campus, Rajamahendravaram, Indian state of Andhra Pradesh. The dust particles were removed by washing with running tap water followed by distilled water, further subjected to shade drying and made into fine powder using domestic blender.

2.3.Sand Bath Assisted synthesis of CDs: This method was adopted with slight modification to synthesize the EHCD's according to the Gudimella et.al [20]. Typically, 5 grams of EH powder was dispersed in 300 mL of distilled water in a round bottom flask. The suspension was placed on a sand bath with magnetic stirring at 180^{o}C and operated for 18 hrs until the reaction mixture turned to dark brown. The resultant solution was centrifugated and filtered with Whatman No.1 filter paper followed by PVDF membrane syringe filters (0.22 µM).

2.4. Synthesis of Fe@EHCD nanocomposites: 5mM of $(FeNo_3)_3$ and EHCD's were taken in 9:1 ratio for the synthesis of Fe@EHCD nanocomposites. Briefly 5 mM of $(FeNo_3)_3$ was dissolved in DH_2O and kept on magnetic stirrer at 70°C. The EHCD's were slowly released into the above solution (flow rate 1mLmin^{-1}) and the reaction mixture turned to dark brown through time. The obtained nanocomposites were centrifuged at 10,000 rpm for 5 minutes at 4°C and the pellet was washed with 70 % of ethanol and dried at 70°C in hot air oven.

2.5. Characterization of Fe@EHCD nanocomposites:

2.5.1. Optical and Fluorescence properties: The absorbance spectrum of EHCDs and Fe@EHCD nanocomposites was analyzed using UV-Vis spectrophotometer (UV-2600) from 200-800 nm wavelength. The fluorescence excitation and emission spectrum of EHCDs was measured using fluorescence spectrophotometer (Perkin Elmer).

2.5.2. Crystalline nature and Zeta potential: The average crystalline size, crystalline nature and zeta potential of Fe@EHCD nanocomposites were evaluated using powder X-ray diffractometer (Bruker) from 0to 120 ° 2θ angle and Zeta potential analyzer (MALVERN) respectively.

2.5.3. Composition and Morphology: The functional groups of EHCDs and Fe@EHCD nanocomposites were evaluated using Fourier Transform Infrared Spectroscopy (FTIR) (Bruker Alpha II) from 500-4000 cm^{-1}. The shape, elemental composition and size distribution of Fe@EHCD nanocomposites were evaluated using Field emission scanning electron microscopy with energy dispersive X-ray spectrometry (FESEM-EDX) (JOEL) and High-resolution transmission electron microscopy (HRTEM) (FEI Tecnai G2, F30).

2.6. Biological activities of Fe@EHCD nanocomposites:

2.6.1. Antimicrobial activity: The antimicrobial activity of Fe@EHCD nanocomposites was tested against four pathogenic bacteria *Staphylococcus aureus* (MTCC 87), *Streptococcus pyogenes* (MTCC 442), *Salmonella enterica typhimurium* (MTCC 98), *Shigella flexneri* (MTCC 1457), and two pathogenic fungal species; *Candida albicans* (MTCC 183), *Aspergillus Niger* (MTCC 282) using Well diffusion and microbroth dilution assays.

In well diffusion assay, the antimicrobial properties of Fe@EHCD nanocomposites were evaluated on Muller Hinton Agar (MHA) and modified MHA with 2% glucose W/methylene blue for bacteria and fungi respectively. Approximately 10^5 CFU/mL of each pathogenic culture was inoculated on agar plates and wells were made using gel puncture. Two different concentrations (1000 and 2000 µg mL^{-1}) of Fe@EHCD nanocomposites (In 5% DMSO) were added into each well. Streptomycin (500 µg mL^{-1}) and Amphotericin B (500 µg mL^{-1}) was used as positive control for bacteria and fungi respectively. Whereas 5% DMSO was used as negative control. The plates were incubated at 37°C for 24 hours and zone of inhibition was calculated in mm. The Micro broth dilution was used to evaluate the Minimum Inhibitory Concentration (MIC) of Fe@EHCD nanocomposites and carried out in 96 well microtiter plates. The concentrations of Fe@EHCD nanocomposites used 1000-3.9 µg mL^{-1} added with two-fold dilution method. The concentration of each pathogen was 10^5 CFU mL^{-1} in LB Broth and 1% TTC solution was added into all the wells. A control was maintained and the microtiter plates were incubated at 37°C for 24 hrs. The MIC was evaluated visually and the change in color of broth (Colorless to red) indicates the presence of bacterial growth[21].

2.6.2. *Invitro* antioxidant activities Fe/EHCD nanocomposites:

The *invitro* antioxidant properties of Fe@EHCD nanocomposites were evaluated using two different methods: DPPH free radical scavenging activity and Ferric reducing antioxidant power assay (FRAP). The various concentrations of Fe@EHCD's (500-2000 µg mL^{-1}) concentrations were added to the 3 x 10^{-5} M of DPPH reagent and FRAP reagent (300mM acetate buffer, 10mM TPTZ in 40mM HCL and 20mM $FeCl_3.6H_2O$ in proportion of 10:1:1) separately. The reaction mixtures were incubated in dark at 25°C and absorbance was read at 517nm and 593nm for DPPH and FRAP respectively.

The percentage of Inhibitory activity/ scavenging activity was estimated as follows:

((A0-A1)/A0) x 100 Formula [1]

A0 = Absorbance of control

A1 = Absorbance of sample

The DPPH and FRAP reagent without sample was used as control and ascorbic acid as standard. The Inhibitory concentration 50 (IC_{50}) was estimated as following formula[21]

IC_{50}= (0.5-b)/a. Formula [2]

2.6.3. *In vitro* anti-inflammatory activities of Fe@EHCD nanocomposites:

The *in vitro* anti-inflammatory effect of Fe@EHCD nanocomposites was assessed by inhibition of protein denaturation, heat induced RBC membrane lysis assay and Inhibition of Proteinase inhibitory activity assays. The concentrations of Fe@EHCD nanocomposites used were 400-2000µg mL^{-1}. Aspirin was used as standard.

In protein denaturation inhibition assay, reaction mixtures composed of phosphate-buffered saline (pH 6.4), 1% bovine serum albumin (BSA), and varying concentrations of Fe@EHCD nanocomposites were incubated at 37°C for 15 minutes, followed by heating at 70°C for an additional 5 minutes. After cooling to room temperature, turbidity was measured at 660nm, with a phosphate buffer solution serving as the control. For the heat-induced haemolysis assay, heparinized chicken blood was centrifuged at 5000 rpm for 5 minutes, and the supernatant was removed. The blood cells were washed three times with an equal volume of physiological saline (0.9% NaCl) and resuspended in 10% PBS (pH 7.4). Reaction mixtures containing the blood suspension, PBS (pH 7.4), and varying concentrations of Fe@EHCD nanocomposites were incubated at 54°C for 20 minutes in a shaking water bath. After centrifugation at 2500 rpm for 5 minutes, the absorbance of the supernatant was read at 540nm, using a phosphate buffer solution as the control. In the proteinase denaturation inhibition assay, reaction mixtures consisting of 0.05mg trypsin, Tris-HCl (pH 7.4), and different concentrations of Fe@EHCD nanocomposites were incubated at 37°C for 5 minutes. Subsequently, 48 µg of casein hydrolysate was added to all reaction mixtures, followed by a further 20-minute incubation at 37°C. The reaction was stopped by adding 70% perchloric acid. After cooling and centrifugation at 3000 rpm for 5 minutes, the absorbance of the supernatant was read at 210nm, with a phosphate buffer solution as the control. Aspirin was used as the standard reference.

The % of inhibition of activity was calculated according to the formula [1].

The IC_{50} value was determined according to the formula [2]

3. Results and Discussion

3.1. Optical and Fluorescence properties: The preliminary confirmation of Fe@EHCD nanocomposite formation was observed by the change of reaction mixture color from yellow to dark brown and which was further evaluated by UV-Vis spectroscopy from 200-800nm wavelength range. The UV-

Vis spectral analysis of EHCDs and Fe@EHCD nanocomposite are depicted in fig.1a. The maximum absorbance of EHCDs was observed at 223 and 259 nm with an extending tail up to UV region and corresponds to π-π* and n-π* transitions respectively [22] Similar studies were also reported by [3, 23]. CDs are effective in reduction of metal/metal oxide nanoparticles than corresponding phytochemicals [24]. In the present study, the FeNPs were reduced by using EHCDs and the maximum absorbance was observed at 216 and 276 nm. Green synthesis of FeNPs using leaves of *Glycosmis mauritiana* and *Phoenix dactylifera* shown absorbance spectrum at 410 and 450nm respectively which are contrast to the present study[25, 26]. The absorbance observed at UV region in this study is may be due to completed reduction and formation of FeNPs. Flourescence is one of the unique property of CDs for applications of a luminescent materials in biomedical field[27]. The EHCDs in the present study shown good fluorescence stability under continuous UV irradiation (365nm) which ensures its efficiency in bioimaging. The excitation of EHCDs was found at 530nm which typically represents the color green depicted in fig.1. b.

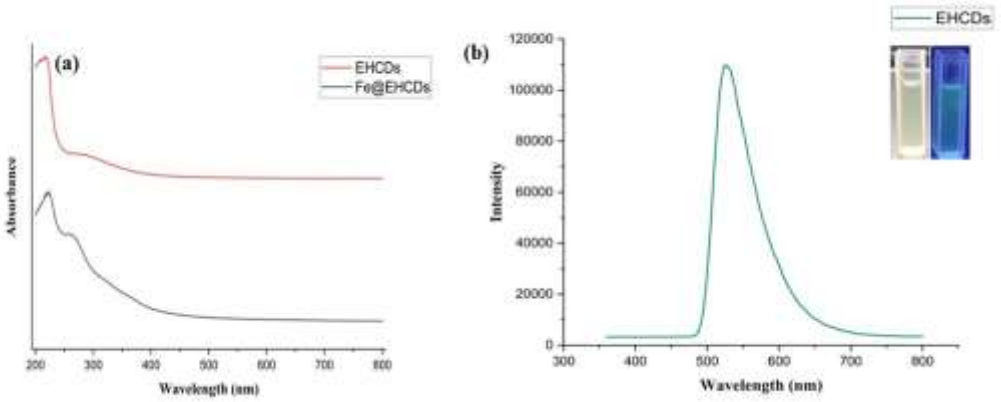

Fig 1. Optical and Fluorescence properties. (a) UV-Visible spectrum of EHCDs and Fe@EHCD nanocomposites (b) Fluorescence excitation of EHCDs at 530nm: the inset shows the color of EHCDs at day light and UV light (365nm).

3.2. Crystalline nature and Zeta potential:

The XRD analysis was carried out to understand the crystalline nature of Fe@EHCD nanocomposites and which was confirmed by appearance of sharp intense peaks represented in fig.2(a). The observed diffraction peaks with 2θ values of 19.34°, 27.28°, 29.87°, 35.67°, 39.53°, 44.94°, 50.36°, 54.32°, 64.50°, and 73.75°corresponds to crystallographic planes of 102, 104, 112, 114, 115, 008, 302, 304, 314, and 137which revealed face cubic centered (fcc) structure of Fe/EHCDs nanocomposites. The Debye-Scherrer equation revealed the average crystalline size of 8nm. Surprisingly the XRD data in the present study consistence with standard JCPDS carbonyl iron card No. 01-070-1926 which is contradictory to the previous studies synthesized FeNPs using green routes [25, 26].

Zeta potential describes the electrokinetic potential and colloidal stability of nanoparticles[28]. In the present study Fe@EHCD nanocomposites shown zeta potential of -5.28mV represented in fig.2b. The zeta potential value between +30 and -30mV considered as colloidal stability of nanoparticles[29].

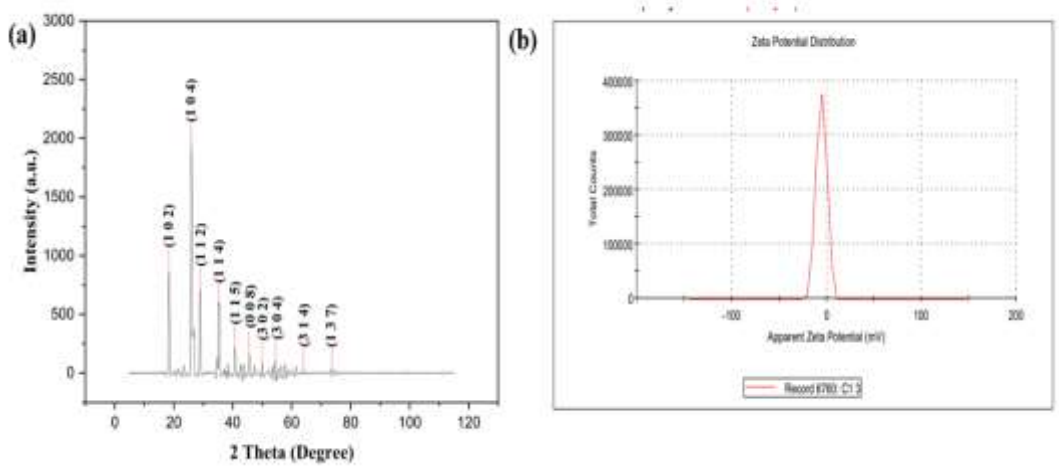

Fig. 2: XRD analysis and Zeta potential (a) XRD spectrum and (b) Zeta potential of Fe@EHCD nanocomposites.

3.3. Composition and Morphology:

The functional groups of EHCD's and the functional groups associated with reduction and capping of of Fe@EHCD nanocomposites were subjected to FTIR analysis from the range of 500-4000 cm^{-1} and the spectra (Fig.3) shows multiple vibrational signals. The EHCD's shows vibrational signals at 3318 cm^{-1} corresponds to strong and broad O-H stretching, 2112cm^{-1} corresponds to weak C≡C stretching, 1634 cm^{-1} corresponds to medium C=C stretching and 509 cm^{-1} corresponds to strong C-I stretching. The Fe@EHCD nanocomposites exhibited minor vibrational stretching at 3735-3621, 2344, 1661, 1535, 1363, 1033 cm^{-1} corresponds to the functional groups O-H stretching (strong) O=C= O stretching (weak), C=C stretching (strong), O-H stretching (medium) and C-N stretching (medium) respectively. A vibrational stretching at 510 cm^{-1} corresponds metal oxide bond. The surface morphology, elemental composition and elemental mapping of Fe@EHCD nanocomposites established using FESEM coupled with EDX (fig.4 (a-c)). The moderate agglomeration and partly spherical shape of nanocomposites were observed in this present study The morphology (shape and size) of Fe@EHCD nanocomposites greatly influenced by the carbon dots participated in the reduction of Fe@EHCD nanocomposites. The EDX spectrum shows characteristic peak of elements Fe (at 0.5kV and 6.5kV) and C (Near to 0kV) with weight percentages 71.93%, 28.07% respectively. The HRTEM analysis was employed to adjudge the particle size distribution and Selected Area Diffraction (SAED) pattern of Fe@EHCD nanocomposites represented in fig.5 (a-c). The SAED pattern revealed monocrystalline particles with an average size of 3.74nm which is contrast to the XRD crystalline size data. The average crystalline grain size must be lesser than the average particle size [30].

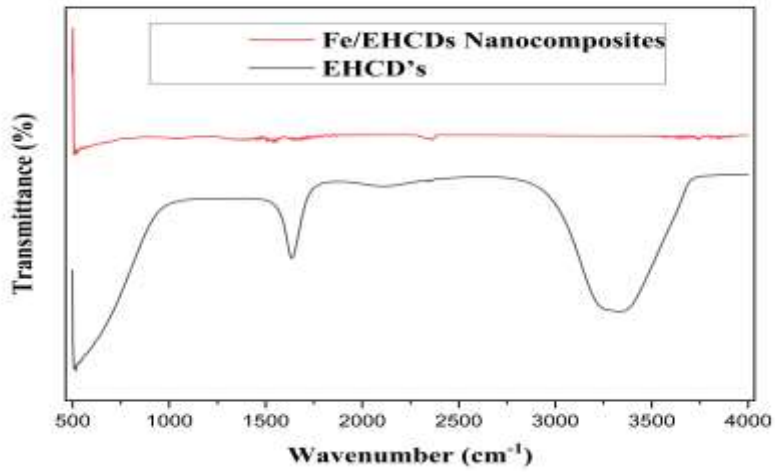

Fig.3.FTIR spectra of EHCD's and Fe@EHCD nanocomposites.

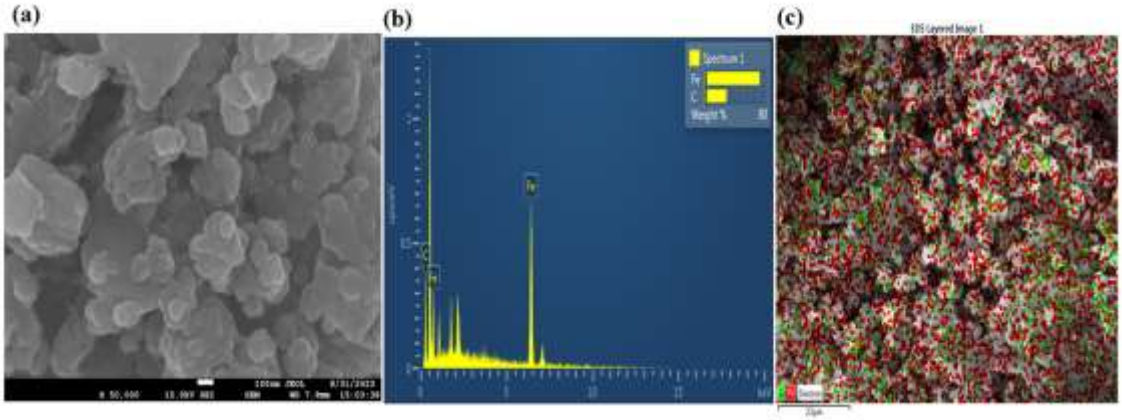

Figure 4: FESEM coupled with EDX analysis of Fe@EHCD nanocomposites, (a) FESEM surface morphology, (b) EDX spectrum (c) Elemental mapping.

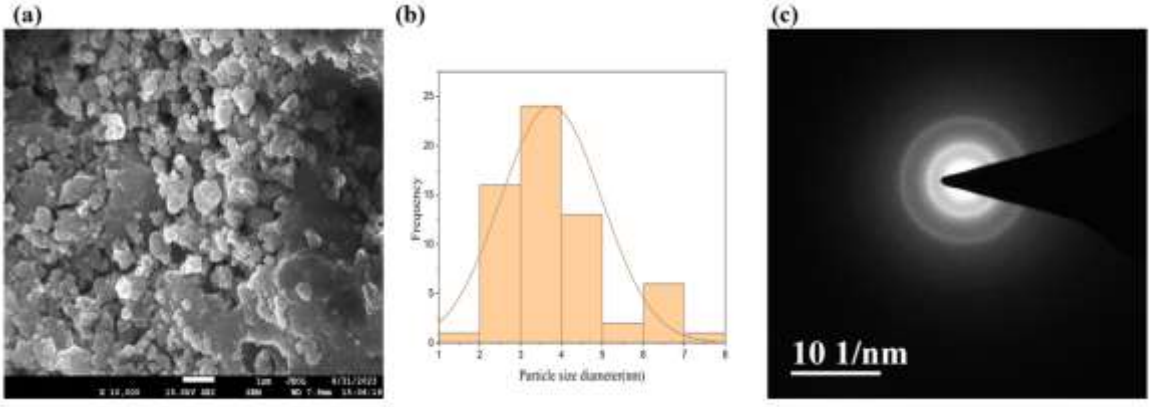

Figure 5: HRTEM Micrograph analysis of Fe@EHCD nanocomposites(a) Morphology b) Particle size distribution (c) SAED pattern.

3.4. Biological activities:

3.4.1. Anti-microbial activity:

Antimicrobial resistance poses a significant worldwide risk, necessitating the development of alternative therapeutics that are both safe for human life and the environment[31]. The field of

nanobiotechnology has paved the way for the creation of novel materials in a sustainable manner. The combination of carbon dots and metals holds great promise as effective materials against microbes. With their small size, the nanocomposites can produce reactive oxygen species (ROS), ultimately resulting in microbial death[32].The antimicrobial efficacy of Fe@EHCD nanocomposites was evaluated using both well diffusion and microbroth dilution methods, as depicted in fig. 6a & b respectively. The results revealed a notable zone of inhibition of 18mm against *Candida albicans* at a concentration of 2000 µg mL^{-1}, with a minimum inhibitory concentration (MIC) of 250 µg mL^{-1}. Furthermore, a moderate zone of inhibition was observed against other tested microbial species. Notably, *Shigella flexneri* exhibited resistance to control (streptomycin), with a zone of inhibition of only 8mm at a concentration of 500 µg mL^{-1}, in contrast to the effectiveness observed against other microbial species. In the present study, the Fe@EHCD nanocomposites exhibited lower zone of inhibition and elevated MIC values against tested microbes, except for *Candida albicans*. These findings highlight the promising antimicrobial activity of Fe@EHCD nanocomposites, particularly against *Candida albicans*, and emphasize the significance of their potential application in combating microbial infections.

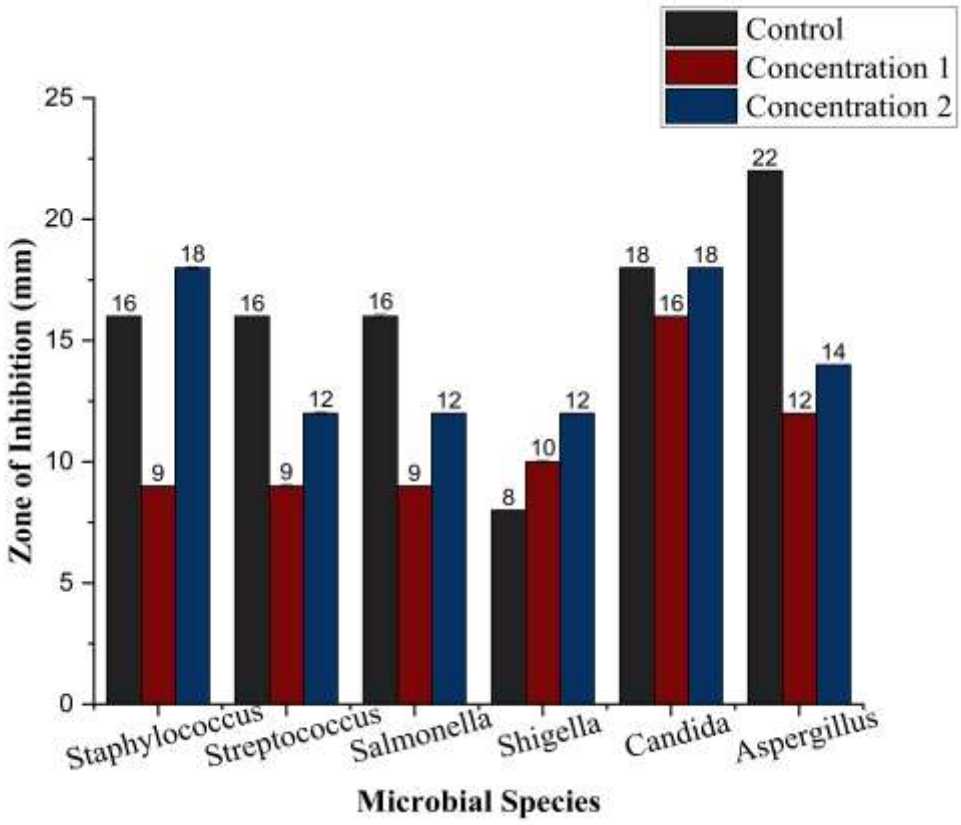

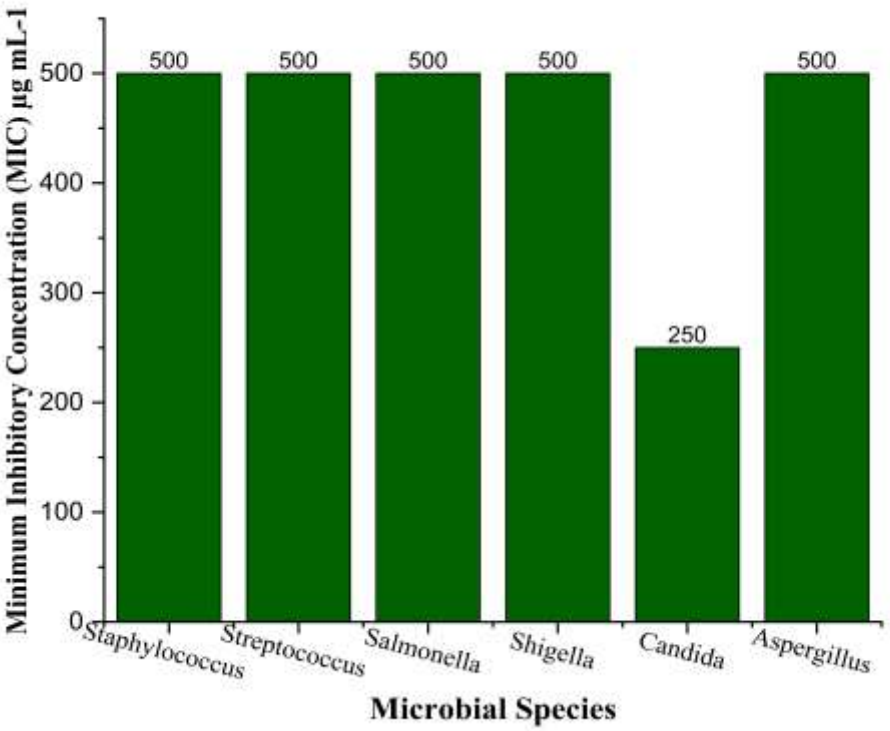

Figure 6: Antimicrobial activity of Fe@EHCD nanocomposites (a) Well diffusion assay, Control (Streptomycin), Concentration 1 (1000 µg mL^{-1}), Concentration 2 (2000 µg mL^{-1}) (b) Minimum Inhibitory concentration.

3.4.2. In vitro antioxidant activity:

Living organisms produce reactive oxygen species (ROS) during the progression of chronic diseases such as cardiovascular conditions, diabetes, neurological disorders, cancer, and respiratory illnesses. ROS is one of the major contributors for degenerative senescence[33]. The antioxidant capabilities of Fe@EHCD nanocomposites were assessed using DPPH free radical scavenging and ferric reducing assays. The concentration-dependent % of activity of these assays are illustrated in fig.7. Both *in vitro* assessments demonstrated potent antioxidant properties, showing maximum inhibition percentages of 62.54% and 69.35% for the DPPH and FRAP assays, respectively, at a concentration of 2000 µg mL^{-1}. Notably, in this study, Fe@EHCD nanocomposites exhibited elevated IC_{50} values, specifically 2075.23 µg mL^{-1} for the DPPH assay and 3962.13 µg mL^{-1} for the FRAP assay. When treated with strong antioxidant compound (Plant extracts/ Carbon dots/ Nanocomposites) the DPPH free radical (Purple color) turns into non-radical form (Yellow color) whereas chromogenic oxidants (TPTZ and ferric ions) in FRAP assay turns into light blue to intense blue color due to reduction of Fe^{3+} to Fe^{2+}. The change in color is directly proportional to the strong antioxidant potential [31][33]. These results underscore the considerable antioxidant efficacy of Fe@EHCD nanocomposites, suggesting their potential as effective agents in combating oxidative stress.

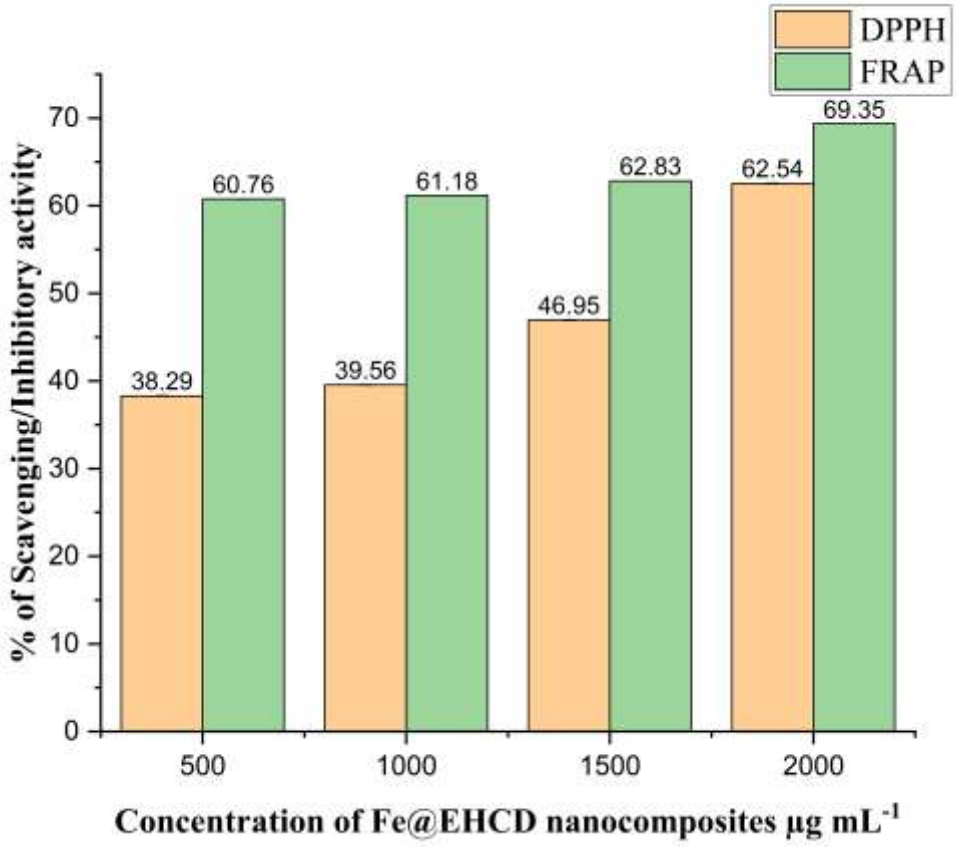

Fig.7. DPPH and FRAP antioxidant activity of Fe@EHCD nanocomposites

3.4.3. *In vitro* anti-inflammatory activities:

Inflammation refers to an immune response triggered by an infection or invasion of pathogens. Conventional steroidal and non-steroidal anti-inflammatory drugs are associated with side effects[33].The anti-inflammatory potential of Fe@EHCD nanocomposites was systematically assessed through three distinct in vitro assays: inhibition of albumin denaturation, inhibition of heat-induced RBC hemolysis, and inhibition of proteinase denaturation. The concentration-dependent percentage of inhibition is elucidated in Figure 8. Notably, among the three assays, Fe@EHCD nanocomposites exhibited significant efficacy in inhibiting albumin denaturation, with a maximum percentage inhibition of 57.30% at a concentration of 2000 µg mL^{-1}. In contrast, inhibition of heat-induced RBC hemolysis and inhibition of proteinase denaturation demonstrated maximum percentage inhibitions of 12.86% and 32.18%, respectively, at the same concentration (fig.8). Despite variations in the percentage of inhibitory activity, the three assays displayed comparable IC_{50} ranges. Specifically, the IC_{50} values were approximately 1061.49 µg mL^{-1} for inhibition of protein denaturation, 1187.17 µg mL^{-1} for inhibition of heat-induced RBC hemolysis, and 1318.72 µg mL^{-1} for inhibition of proteinase denaturation. These findings underscore the noteworthy anti-inflammatory properties of Fe@EHCD nanocomposites across diverse mechanisms, suggesting their potential as effective agents in mitigating inflammatory responses.

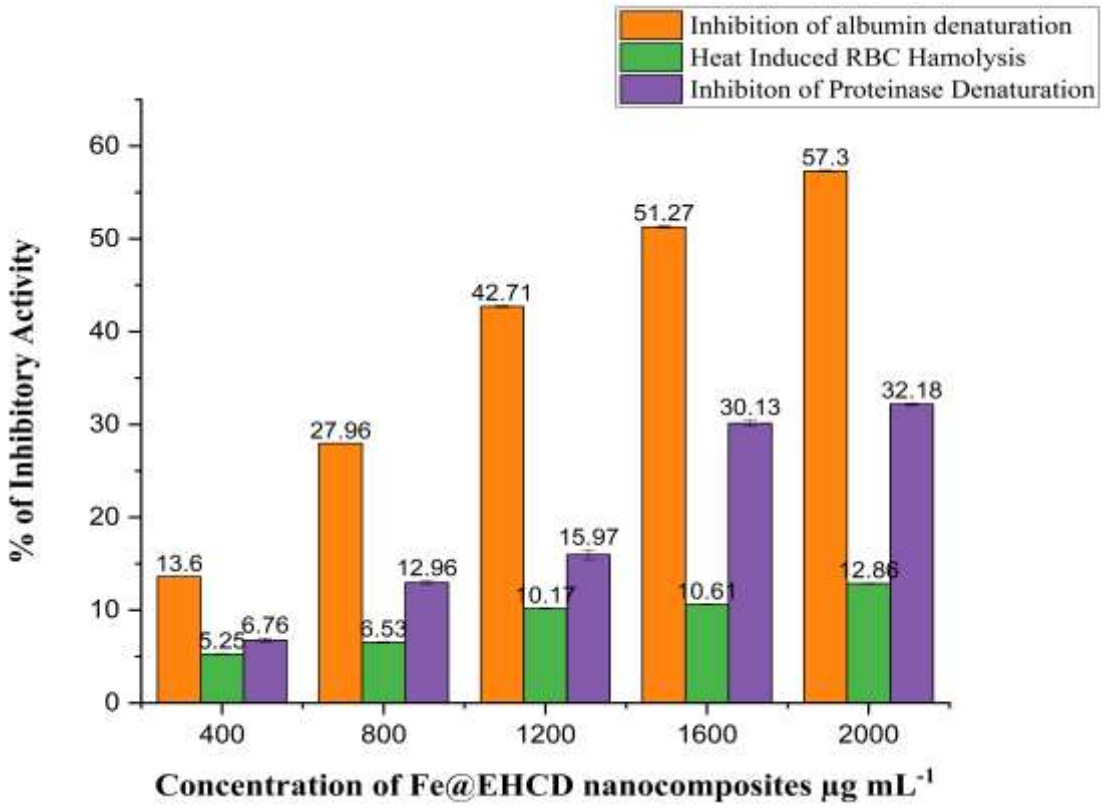

Figure 8: ***In vitro*** **anti-inflammatory activities of Fe@EHCD nanocomposites**

Conclusion:

In this study, carbon dots were meticulously synthesized from the Euphorbia heterophylla plant, employing a sand bath-assisted method. The confirmation of EHCD synthesis was established through UV-Vis and FTIR analyses, which examined absorbance and functional groups, respectively. Remarkably, the study observed the complete reduction of Fe nanoparticles (FeNPs) facilitated by the CDs, given their diminutive size (<10nm). The synthesized FeNPs using EHCDs exhibited a particle size distribution ranging between 2-8nm and a partially spherical shape. Of the various biological properties assessed, the in vitro antioxidant characteristics stood out prominently compared to antimicrobial and anti-inflammatory properties. This distinction was attributed to the maximum percentage of inhibition exhibited at lower concentrations of Fe@EHCD nanocomposites. Consequently, these nanocomposites emerge as particularly well-suited for alleviating oxidative stress associated with various human ailments.

Funding Statement: The present work was funded by Government College (Autonomous), Rajamahendravaram under Research Project Seed Money Policy with sanction order No: 004/GCRJY/Acad.Cell/ Research Funding/2022, dated. 25.04.2023.

Abbreviations; CD's: Carbon Dots; Fe@EHCD's: Iron *Euphorbia heterophylla* Carbon Dots nanocomposites; FTIR: Fourier transform infrared spectroscopy; XRD: X-ray diffraction; SEM: Scanning electron microscope; TEM: Transmission electron microscope;

Acknowledgements The authors also thankful to Central Instrumentation Laboratory, Government College (Autonomous), Rajamahendravaram, for providing necessary facilities for conducting this research work.

Author Contribution BN was involved in the supervision and conceptualization of the project. KSLK and DK were responsible for methodology, investigation, resources, and writing the original draft manuscript.

Data Availability Correspondence and requests for materials should be addressed to BN.

Declarations

Competing interests The authors declare no competing interests.

Conflict of Interest The authors declare no competing interests.

Ethics Approval and Consent to Participate Not applicable.

Consent for Publication Not applicable.

Research Involving Humans and Animals Statement The article does not contain any studies involving human participants and animals performed by any of the authors.

Informed Consent Not Applicable

REFERENCES:

1. Zhang, F. (2017). Grand Challenges for Nanoscience and Nanotechnology in Energy and Health. *Frontiers in Chemistry*, *5*(October), 1–6. https://doi.org/10.3389/fchem.2017.00080
2. Abu Salha, B., Saravanan, A., Maruthapandi, M., Perelshtein, I., & Gedanken, A. (2023). Plant-Derived Nitrogen-Doped Carbon Dots as an Effective Fertilizer for Enhanced Strawberry Growth and Yield. *ACS ES&T Engineering*, *3*(8), 1165–1175. https://doi.org/10.1021/acsestengg.3c00046
3. Prathap, N., Balla, P., Shivakumar, M. S., Periyasami, G., Karuppiah, P., Ramasamy, K., & Venkatesan, S. (2023). Prosopis juliflora hydrothermal synthesis of high fluorescent carbon dots and its antibacterial and bioimaging applications. *Scientific Reports*, *13*(1), 1–11. https://doi.org/10.1038/s41598-023-36033-3
4. Barros, M. R., da Silva, L. P., Menezes, T. M., Garcia, Y. S., & Neves, J. L. (2021). Efficient tyrosinase nano-inhibitor based on carbon dots behaving as a gathering of hydrophobic cores and key chemical group. *Colloids and Surfaces B: Biointerfaces*, *207*(July), 112006. https://doi.org/10.1016/j.colsurfb.2021.112006
5. Nizam, N. U. M., Hanafiah, M. M., Mahmoudi, E., & Mohammad, A. W. (2023). Synthesis of highly fluorescent carbon quantum dots from rubber seed shells for the adsorption and photocatalytic degradation of dyes. *Scientific Reports*, *13*(1), 1–17. https://doi.org/10.1038/s41598-023-40069-w
6. Jing, H. H., Bardakci, F., Akgöl, S., Kusat, K., Adnan, M., Alam, M. J., … Sasidharan, S. (2023). Green Carbon Dots: Synthesis, Characterization, Properties and Biomedical Applications. *Journal of Functional Biomaterials*, *14*(1). https://doi.org/10.3390/jfb14010027
7. Singh, P., Arpita, Kumar, S., Kumar, P., Kataria, N., Bhankar, V., … Khoo, K. S. (2023). Assessment of biomass-derived carbon dots as highly sensitive and selective templates for the sensing of hazardous ions. *Nanoscale*, *15*(40), 16241–16267. https://doi.org/10.1039/D3NR01966G
8. Huang, X., Liu, J., Zhao, B., Bai, Y., Peng, Z., Zhou, J., … Zhang, C. (2022). One-step Synthesis of Biomass-Based Carbon Dots for Detection of Metal Ions and Cell Imaging. *Frontiers in Energy Research*, *10*(March), 1–9. https://doi.org/10.3389/fenrg.2022.871617
9. Fan, J., Kang, L., Cheng, X., Liu, D., & Zhang, S. (2022). Biomass-Derived Carbon Dots and Their Sensing Applications. *Nanomaterials*, *12*(24). https://doi.org/10.3390/nano12244473
10. Ashok Kumar, S., Dheeraj Kumar, M., Saikia, M., Renuga Devi, N., & Subramania, A. (2023). A review on plant derived carbon quantum dots for bio-imaging. *Materials Advances*, *4*(18), 3951–3966. https://doi.org/10.1039/d3ma00254c
11. Varsha Raveendran, P. T., & Renuka, N. K. (2022). Carbon dots as a sustainable alternative to plant extracts for the green synthesis of noble metal nanoparticles. *Environmental Nanotechnology, Monitoring & Management*, *18*, 100676.

https://doi.org/https://doi.org/10.1016/j.enmm.2022.100676

12. Tonelli, F. M. P., Silva, C. S., Delgado, V. M. S., & Tonelli, F. C. P. (2023). Algae-based green AgNPs, AuNPs, and FeNPs as potential nanoremediators. *Green Processing and Synthesis*, *12*(1). https://doi.org/10.1515/gps-2023-0008
13. Lingaraju, K., Naika, H. R., Nagaraju, G., & Nagabhushana, H. (2019). Biocompatible synthesis of reduced graphene oxide from Euphorbia heterophylla (L .) and their in-vitro cytotoxicity against human cancer cell lines. *Biotechnology Reports*, *24*, e00376. https://doi.org/10.1016/j.btre.2019.e00376
14. Atarod, M., Nasrollahzadeh, M., & Sajadi, S. M. (2016). Journal of Colloid and Interface Science Euphorbia heterophylla leaf extract mediated green synthesis of Ag / TiO 2 nanocomposite and investigation of its excellent catalytic activity for reduction of variety of dyes in water. *JOURNAL OF COLLOID AND INTERFACE SCIENCE*, *462*, 272–279. https://doi.org/10.1016/j.jcis.2015.09.073
15. Tajbakhsh, M., Alinezhad, H., Nasrollahzadeh, M., & Kamali, T. A. (2016). Green synthesis of the Ag/HZSM-5 nanocomposite by using Euphorbia heterophylla leaf extract: A recoverable catalyst for reduction of organic dyes. *Journal of Alloys and Compounds*. https://doi.org/10.1016/j.jallcom.2016.05.278
16. Lingaraju, K., Naika, H. R., Nagabhushana, H., & Nagaraju, G. (2018). Author ' s Accepted Manuscript. *Biocatalysis and Agricultural Biotechnology*. https://doi.org/10.1016/j.bcab.2018.10.011
17. Kasrina, K., & Zukmadini, A. Y. (n.d.). Green synthesis of Co 3 O 4 nanoparticles using Euphorbia heterophylla L . leaves extract : characterization and photocatalytic activity Green synthesis of Co 3 O 4 nanoparticles using Euphorbia heterophylla L . leaves extract : characterization and photo. https://doi.org/10.1088/1757-899X/509/1/012105
18. Oktri, N., Dewi, M., & Yulizar, Y. (2020). ScienceDirect Euphorbia heterophylla L . Leaf Extract-Mediated Synthesis of MnO 2 Nanoparticles and Its Characterization. *Materials Today: Proceedings*, *22*, 199–204. https://doi.org/10.1016/j.matpr.2019.08.088
19. Lingaraju, K., Naika, H. R., Nagabhushana, H., Jayanna, K., & Devaraja, S. (2020). Biosynthesis of Nickel oxide Nanoparticles from Euphorbia heterophylla (L .) and their biological application. *Arabian Journal of Chemistry*, *13*(3), 4712–4719. https://doi.org/10.1016/j.arabjc.2019.11.003
20. Gudimella, K. K., Appidi, T., Wu, H. F., Battula, V., Jogdand, A., Rengan, A. K., & Gedda, G. (2021). Sand bath assisted green synthesis of carbon dots from citrus fruit peels for free radical scavenging and cell imaging. *Colloids and Surfaces B: Biointerfaces*, *197*(September 2020), 111362. https://doi.org/10.1016/j.colsurfb.2020.111362
21. Pangi, V. N., Marukurti, A., Reddy, A. M., & Medapalli, S. R. (2023). Synthesis of Biogenic Silver Nanoparticles (bAgNPs) Using Leaf Extract of Mirabilis jalapa and Evaluation of Anti-vibriocidal, Anti-oxidant properties and Cytotoxicity. *BioNanoScience*, *13*(2), 376–392. https://doi.org/10.1007/s12668-023-01060-x
22. Sharma, A., Gadly, T., Gupta, A., Ballal, A., Ghosh, S. K., & Kumbhakar, M. (2016). Origin of Excitation Dependent Fluorescence in Carbon Nanodots. *Journal of Physical Chemistry Letters*, *7*(18), 3695–3702. https://doi.org/10.1021/acs.jpclett.6b01791
23. Bajpai, S. K., D'Souza, A., & Suhail, B. (2019). Blue light-emitting carbon dots (CDs) from a milk protein and their interaction with Spinacia oleracea leaf cells. *International Nano Letters*, *9*(3), 203–212. https://doi.org/10.1007/s40089-019-0271-9
24. Jin, J. C., Xu, Z. Q., Dong, P., Lai, L., Lan, J. Y., Jiang, F. L., & Liu, Y. (2015). One-step synthesis

of silver nanoparticles using carbon dots as reducing and stabilizing agents and their antibacterial mechanisms. *Carbon*, *94*, 129–141. https://doi.org/10.1016/j.carbon.2015.05.084

25. Batool, F., Iqbal, M. S., Khan, S. U. D., Khan, J., Ahmed, B., & Qadir, M. I. (2021). Biologically synthesized iron nanoparticles (FeNPs) from Phoenix dactylifera have anti-bacterial activities. *Scientific Reports*, *11*(1), 1–9. https://doi.org/10.1038/s41598-021-01374-4
26. Amutha, S., & Sridhar, S. (2015). Green synthesis of magnetic iron oxide nanoparticle using leaves of Glycosmis mauritiana and their antibacterial activity against human pathogens. *Journal of Innovations in Pharmaceutical and Biological Sciences (JIPBS)*, *5*(2), 22–26.
27. Raveendran, V., & Kizhakayil, R. N. (2021). Fluorescent Carbon Dots as Biosensor, Green Reductant, and Biomarker. https://doi.org/10.1021/acsomega.1c03481
28. İlhan, M., Gültekin, H. E., Rençber, S., Şenyiğit, Z., & Aydın, H. H. (2022). Chapter 12 - Aquasomes: a novel platform for drug delivery. In A. K. Nayak, M. S. Hasnain, T. M. Aminabhavi, & V. P. Torchilin (Eds.), *Systems of Nanovesicular Drug Delivery* (pp. 191–206). Academic Press. https://doi.org/https://doi.org/10.1016/B978-0-323-91864-0.00020-6
29. Das, P., & Das, M. K. (2022). Chapter 4 - Production and physicochemical characterization of nanocosmeceuticals. In M. K. Das (Ed.), *Nanocosmeceuticals* (pp. 95–138). Academic Press. https://doi.org/https://doi.org/10.1016/B978-0-323-91077-4.00006-5
30. Shiraishi, M., & Inagaki, M. (2003). Chapter 10 - X-ray Diffraction Methods to Study Crystallite Size and Lattice Constants of Carbon Materials. In E. YASUDA, M. INAGAKI, K. KANEKO, M. ENDO, A. OYA, & Y. TANABE (Eds.), *Carbon Alloys* (pp. 161–173). Oxford: Elsevier Science. https://doi.org/https://doi.org/10.1016/B978-008044163-4/50010-3
31. Perveen, S., Nadeem, R., Afzal, N., Al-mijalli, S. H., & Iqbal, M. (2022). Green synthesis of iron (Fe) nanoparticles using Plumeria obtusa extract as a reducing and stabilizing agent : Antimicrobial , antioxidant and biocompatibility studies. *Arabian Journal of Chemistry*, *15*(5), 103764. https://doi.org/10.1016/j.arabjc.2022.103764
32. Wang, P., Song, Y., Mei, Q., Dong, W.-F., & Li, L. (2022). Sliver nanoparticles@carbon dots for synergistic antibacterial activity. *Applied Surface Science*, *600*, 154125. https://doi.org/https://doi.org/10.1016/j.apsusc.2022.154125
33. Nahari, M. H., Ali, A. Al, Asiri, A., Mahnashi, M. H., Shaikh, I. A., Shettar, A. K., & Hoskeri, J. (2022). Green Synthesis and Characterization of Iron Nanoparticles Synthesized from Aqueous Leaf Extract of Vitex leucoxylon and Its Biomedical Applications.